Lab Notes

Editors
Thomas M. Moses | Shane F. McClure

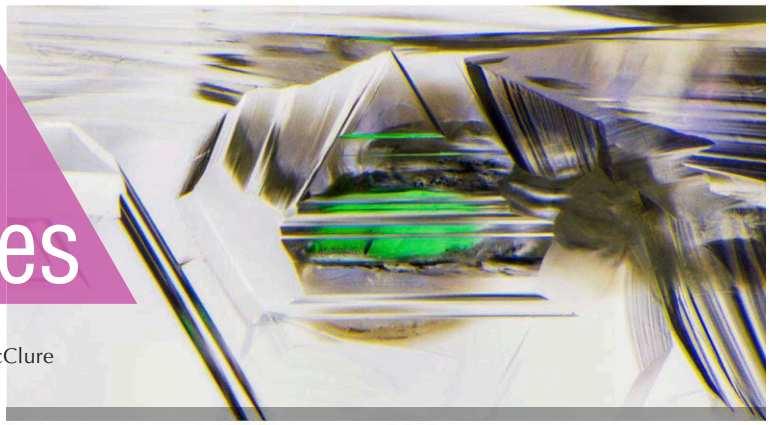

DIAMOND

Blue "Graining" in Green-Yellow Diamond

It is not uncommon for fancy-color diamonds to possess uneven color distribution. This is generally seen as diffuse concentrations of color that may arise from changes in growth environment, natural or artificial irradiation, or as linear graining. Color zoning from radiation is often diffuse and blue or green in color, whereas graining exists as sharp distinct lines and is typically brown, pink, or yellow in color. Blue color zones resembling graining, however, were recently observed in a 1.50 ct Fancy Intense green-yellow diamond (figure 1) at the Carlsbad laboratory.

The diamond was type IaAB and showed clear spectroscopic evidence of both high-pressure, high-temperature (HPHT) treatment and artificial irradiation. Under magnification, the stone showed reflective cubic graining and strong green luminescence with fiber-optic lighting. When immersed, it revealed a blue colored crown (created during the artificial radiation color treatment) and a yellow pavilion. This type of color zoning is unusual, as artificial radiation is typically done on the pavilion of faceted diamonds, not the crown. When viewed under magnification with diffused light, the stone displayed yellow and brown graining as well as peculiar blue grain lines (figure 2). Graining is associated with regions of planar lattice deformities, or plastic deformation that formed when the diamond was deep in the earth's mantle. Colored graining occurs when regions of plastic deformation coexist with clusters of lattice vacancies or complex nitrogen defects.

Figure 1. The 1.50 ct Fancy Intense green-yellow round brilliant diamond as seen from the crown.

Blue graining has rarely been seen as a cause of blue coloration in treated or untreated diamonds. Blue color is almost always a result of trapped boron atoms within the diamond lattice (type IIb; usually with a uniform color distribution) or exposure to natural or artificial radiation (usually with a patchy color). Given that no boron impurities were seen in the infrared spectra, radiation damage was most likely the cause of this blue "graining."

Figure 2. Blue "graining" was seen in this 1.50 ct HPHT-treated and irradiated Fancy Intense green-yellow diamond. Note the dark yellow graining also visible in this image. Field of view 4.90 mm.

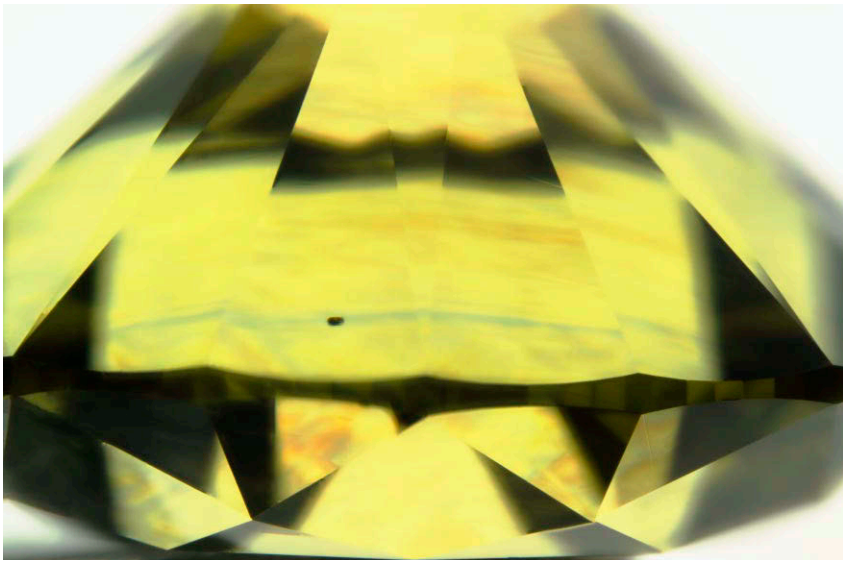

Editors' note: All items were written by staff members of GIA laboratories.

GEMS & GEMOLOGY, Vol. 56, No. 4, pp. 516–525.

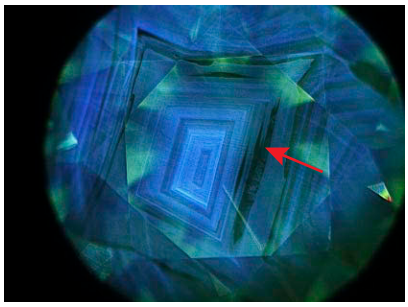

Figure 3. DiamondView imaging showed strong blue fluorescence and inert zones corresponding to nitrogen-rich and nitrogen-poor areas, respectively. The inert zone shown by the red arrow correlated with the blue "graining" seen in figure 2.

When diamonds are analyzed with DiamondView, nitrogen-rich areas often show strong blue fluorescence due to N3 defects while lower-nitrogen areas (type IIa) are sometimes inert. The diamond showed strong blue fluorescence in an octahedral growth pattern with streaky inert patches (figure 3). These inert streaks appeared to correspond with the location of the blue zone, as seen under magnification in diffused light. When viewed through the pavilion, the zoning on the crown has a grain-like appearance (figure 2).

We propose that the blue zone with a grain-like appearance formed during artificial irradiation treatment within a region of diamond containing very low nitrogen impurities. Initially, this stone likely had a brown color. HPHT treatment then influenced the bodycolor by destroying the initial brown color before creating most of the yellow component as well as green luminescence. When artificial irradiation treatment followed, we believe that vacancies were created in higher concentrations within the low-nitrogen regions to create the blue color zone. This is similar to the way type IIa diamonds are HPHT treated and irradiated to a blue color. This stone is a fine illustration of how inherent heterogeneities of impurity distribution within diamond can be differentially affected by treatments.

Britni LeCroy and Virginia A. Schwartz

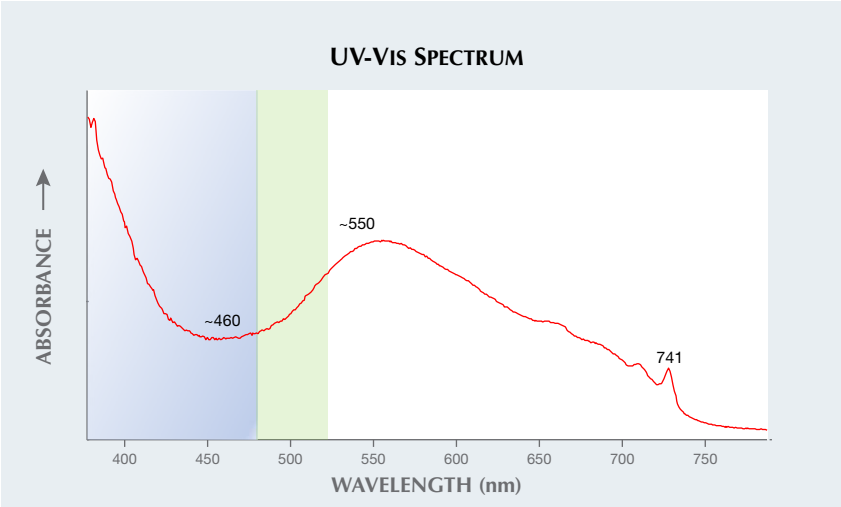

Figure 5. UV-visible spectrum collected from the 0.53 ct diamond showing the ~550 nm absorption band and blue transmission window at ~460 nm. Also observed is the GR1 peak at 741 nm.

Irradiated Blue Diamond

Blue is a very desirable color for diamond. A rare type of blue to violet hydrogen-rich diamond came from the recently closed Argyle mine in Australia ("Gray-to-blue-to-violet hydrogen-rich diamonds from the Argyle mine, Australia," C.H. van der Bogert et al., Spring 2009 *G&G*, pp. 20–37). Prior to the discovery of the Argyle mine, *G&G* reported on a rare 4.28 ct bluish gray diamond with the 550 nm band feature (R. Crowningshield, "Developments and Highlights at GIA's Lab in New York," Fall 1969 *G&G*, pp. 89–90).

Figure 4. The 0.53 ct Fancy Light blue pear-shaped diamond. The face-up color in this image does not appear blue or match the colorimeter image in figure 7 (right).

Recently submitted to the New York laboratory for identification was a 0.53 ct pear-shaped diamond graded as Fancy Light blue on GIA's color grading system (figure 4).

Gemological features typical of natural pink type Ia diamonds were observed under the microscope, including very strong graining or glide planes with a pink color. IR spectroscopy confirmed that this is a type Ia diamond. The unusual graining (haziness) seen in figure 4 contradicts the blue color of this diamond.

A UV-visible absorption spectrum collected from this diamond showed a broad band at about 550 nm, typical for this type of diamond and the pink color attributed to it (resulting from plastic deformation of the crystal lattice during growth or post-growth). A GR1 (general radiation damage) peak at about 741 nm was also observed. This radiation damage is responsible for the green and blue colors observed in some diamonds, both naturally colored and treated (figure 5).

This is a very unusual combination of spectral features in the same diamond. While the strong 550 nm band absorption creating a strong blue

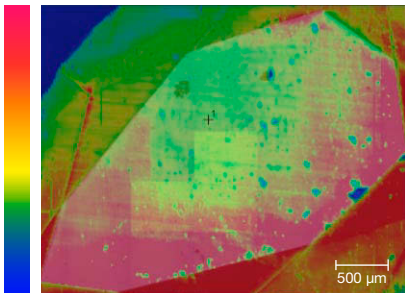

Figure 6. GR1 radiation damage (red) is concentrated on one side of the diamond table facets.

Figure 7. GIA colorimeter images captured the original Fancy Light pinkish purple color (left) and the treated Fancy Light blue color (right) of the 0.53 ct pear-shaped diamond.

transmission window at ~460 nm was responsible for the pink color, the relatively strong GR1 absorption and its side band caused the near-violet color. When mapped with a Raman photoluminescence microscope, this GR1 radiation damage could be seen concentrated on one side of the diamond (figure 6). This concentration of radiation damage, in conjunction with the absorption spectroscopy and gemological features, enabled the confident determination that this diamond had been artificially irradiated to create the desirable blue color. This is a great example of color engineering. Subsequent to this determination, a GIA records query search revealed that this diamond had a previous report with a Fancy Light pinkish purple color grade (figure 7).

Paul Johnson and Surjit Dillon Wong

Large Type IIa Diamond from Arkansas, USA

The GIA lab in Carlsbad recently had the opportunity to examine a truly "all-American" diamond. The 1.16 ct near-colorless cushion-cut stone was submitted for a grading report along with a certificate from Crater of Diamonds State Park in Arkansas, USA, indicating it was cut from a 2.73 ct rough diamond mined in July 2020 by William Dempsey. The diamond was reported to have been cut and polished domestically in North Dakota (figure 8). It was ultimately graded as H color (near colorless) with SI_1 clarity (due to an internal feather). Crater of Diamonds State Park is the only feedig diamond mine in the world where anyone with a prospector's spirit can search in hopes of finding a true gem (Summer 2020 Gem News International, "Finders, keepers: Field trip to Crater of Diamonds, USA," pp. 311–314). At 2.73 ct, the rough stone was exceptionally large for an Arkansas diamond, most of which come in significantly under 1 carat.

Researchers at GIA were excited to study this unique stone, especially with the prospect of analyzing inclusions that might shed light on the geological history of the Arkansas diamond deposit. However, the diamond turned out to be fairly clean with no crystalline inclusions. Somewhat unexpectedly, FTIR spectroscopy revealed the stone to be a type IIa diamond with no measurable nitrogen impurities. Type IIa diamonds are extremely rare among natural diamonds, and some have even been shown to grow much deeper in the earth than most type I diamonds (E.M. Smith et al., "Large gem diamonds from metallic liquid in Earth's deep mantle," *Science*, Vol. 354, No. 6318, pp. 1403–1405). The lack of inclusions in the stone was consistent with its type IIa character. Imaging with the DiamondView instrument showed relatively even blue fluorescence. Photoluminescence spectroscopy confirmed the natural origin of the diamond.

Discovering a type IIa gem diamond is remarkable enough, but uncovering one from a source in the United States, where few diamonds occur, is definitely a noteworthy event.

Aaron C. Palke and Christopher M. Breeding

Figure 8. A 1.16 ct type IIa diamond recovered in 2020 from Crater of Diamonds State Park in Arkansas.

Artificial GLASS Imitating a Paraíba Tourmaline

Recently the Carlsbad laboratory examined two transparent bluish green prisms for identification service (figure 9). The submitted prisms weighed 1.91 ct and 1.92 ct and contained eye-visible clusters of reflective brownish metallic crystal inclusions along with small cavities and minor abrasions. At first glance, these stones resembled either Paraíba tourmaline with copper inclusions or possibly emerald with pyrite inclusions.

Standard gemological testing revealed a single refractive index of 1.50 and a hydrostatic specific gravity of 2.43. Both stones fluoresced weak green to long-wave UV light and weak to medium green to short-wave UV light. Although the six-sided, trigonal prisms had well-formed "crys-

Figure 9. These two pieces of glass with copper inclusions, weighing 1.91 and 1.92 ct, appear to have been manufactured to imitate natural copper-bearing Paraíba tourmaline crystals.

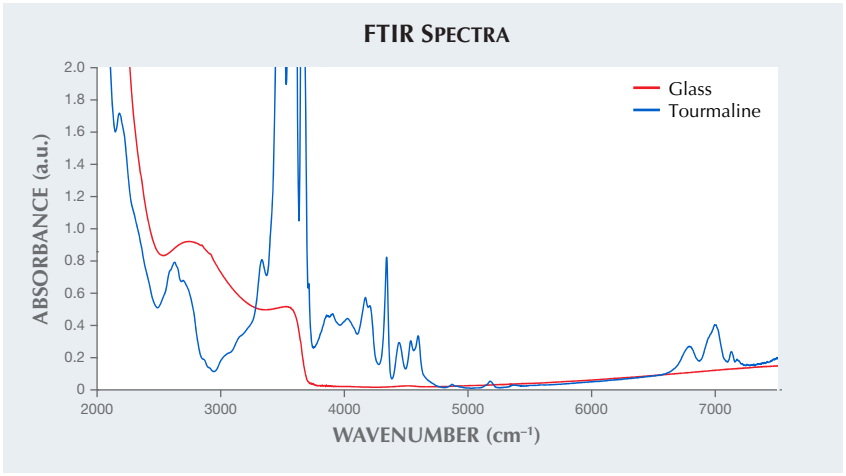

Figure 11. The FTIR spectrum of one of the glass imitations of tourmaline (red trace) was consistent with manmade glass, while the FTIR spectrum for tourmaline (blue trace) is distinctly different.

tal-like" shapes resembling tourmaline, the refractive index ruled out that material.

Microscopic examination with fiber-optic lighting showed trapped gas bubbles, flow structure, and a distinct boundary where two types of glasses, with and without metallic inclusions, were fused together. Areas of encapsulated glass exhibited a light yellow bodycolor and contained geometric metallic crystals and gas bubbles (figure 10). Due to the mixture of the fused glasses, it was obvious that the prisms were manmade.

Infrared spectroscopy confirmed our identification of manmade glass. The FTIR spectrum for manmade glass is very different than that of tourmaline (see figure 11). Further testing with EDXRF showed the presence of Cu, consistent with the copper color of the minute metallic crystal inclusions.

Figure 10. Areas of encapsulated goldstone glass exhibited a light yellow bodycolor and contained geometric copper crystals and gas bubbles. Field of view 3.52 mm.

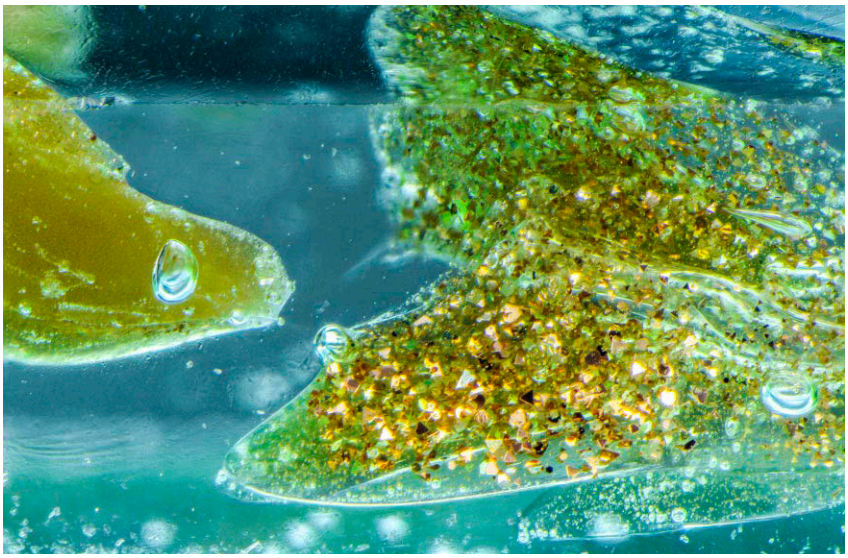

The rough "crystal-like" shape and fusion of two glass types, one with metallic inclusions and one without, present a more complicated type of manmade glass product. This sort of glass imitation using copper platelets to simulate a natural stone has been documented (see E.J. Gübelin and J.I. Koivula, *Photoatlas of Inclusions in Gemstones*, Vol. 1, 2005, Opinio Publishers, Basel, Switzerland, p. 433). The polish lines seen on the surfaces of both glasses clearly indicate that these were faceted to resemble a natural rough stone, and the trigonal outline and elongate shape suggest the goal was to imitate tourmaline, which has a similar appearance. The copper inclusions and neon bluish green color would further indicate that the manufacturer intended to imitate Paraíba-type tourmaline.

During this same time these glass imitations were examined, a natural copper-bearing tourmaline (figure 12) from Brazil was also submitted for a colored stone identification and origin service. This stone was notable because it had rare natural dendritic copper inclusions (figure 13) that the submitted glass imitation attempted to mimic.

It is unusual to see manmade glass cut to imitate a natural rough crystal with eye-visible inclusions. Paraíba tourmaline is one of the most expensive varieties of tourmaline and

Figure 12. Paraíba tourmaline with copper inclusions.

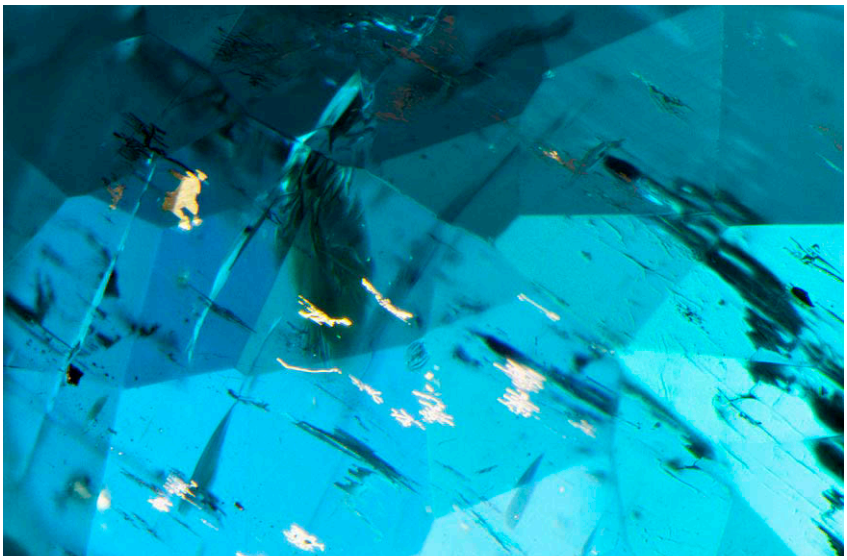

Figure 13. Native copper inclusions in natural Paraíba tourmaline. Field of view 2.82 mm.

well sought after since its discovery in the 1980s. These pieces of man-made glass were certainly interesting from a gemological perspective to demonstrate the variety of creative ways imitation gems are produced.

Amy Cooper, Jamie Price, and Heidi Breitzmann

Chromite Inclusions in Green Common OPAL

Recently the Carlsbad laboratory examined a mottled grayish green partially polished rough stone for identification services. The stone measured 21.01 × 16.13 × 15.50 mm and weighed 28.16 ct (figure 14). The stone showed a vitreous luster and prominent reddish orange staining in surface-reaching fractures and cavities.

Standard gemological testing revealed a refractive index of 1.450 measured on a polished flat surface and a specific gravity of 2.07 obtained hydrostatically. No play-of-color was

Figure 14. This 28.16 ct polished rough dark green common opal contained inclusions of chromite and is colored by chromium.

Figure 15. The chromite inclusions within the green common opal. Field of view 0.95 mm.

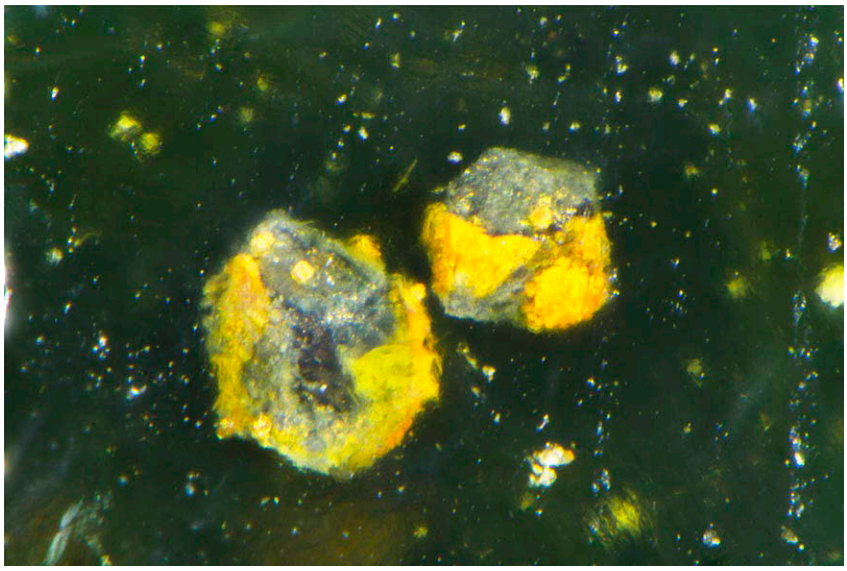

observed, and all properties were consistent with common opal. Weak chromium lines were seen with the handheld spectroscope as well as a weak pink Chelsea color filter reaction. Microscopic analysis using fiber-optic lighting showed minute mineral grains scattered throughout the opal. Several well-formed black opaque octahedral inclusions with yellow staining (figure 15) were confirmed by Raman spectroscopy to be predominantly chromite ($FeCr_2O_4$), a member of the spinel group (C. Klein and B. Dutrow, *The Manual of Mineral Science*, 23rd ed., 2007, pp. 387–388).

Additional information on the chromite inclusions and the green bodycolor of the opal was collected by further advanced testing with LA-ICP-MS (table 1) and Vis-NIR (figure 16). The visible-range spectrum shows a broad absorption band centered at 610 nm and a smaller band at 680 nm, which may result from minute inclusions of chromium-colored serpentine (E. Fritsch et al., "Cr^{3+}-green common opal from Turnali, north-eastern Turkey," *32nd International Gemmological Conference*, Interlaken, Switzerland, 2011, pp. 165–166). LA-ICP-MS trace element chemistry showed the black inclusions were predominantly a mixture of magnesiochromite (24.19 mol.%), chromite (42.94 mol.%), hercynite ($FeAl_2O_4$, 17.99 mol.%), and spinel ($MgAl_2O_4$, 10.12 mol.%). ICP data showed a high amount of chromium ranging from 936–1110 ppmw with an average of 1042 ppmw.

Although the location or geological occurrence of this particular sample is unknown, a previous publication on Turkish green common opal colored by Cr^{3+} discussed the occurrence in deposits of serpentinized peridotite with the color being attributed to minute inclusions of chromium-colored serpentine. This interesting common opal was a welcome gem material to study in the GIA lab.

Amy Cooper, Maxwell Hain, and Ziyin Sun

TABLE 1. LA-ICP-MS data of the inclusions in the green opal revealing they were consistent with the spinel group mineral chromite.

Oxides (wt.%)	Laser spot 1	Laser spot 2	Laser spot 3
MgO	7.32	6.99	7.38
SiO_2	0.02	0.38	0.05
Al_2O_3	14.39	14.64	14.21
TiO_2	0.04	0.04	0.04
Cr_2O_3	51.42	50.85	51.67
MnO	0.33	0.33	0.33
FeO[a]	22.55	23.60	22.54
Fe_2O_3	3.03	2.36	3.12
Others	0.89	0.80	0.64
Total	100.00	100.00	100.00
Atomic proportions on the basis of 4 oxygen atoms			
Mg	0.3639	0.3470	0.3662
Mn	0.0093	0.0094	0.0093
Fe^{2+}	0.6286	0.6572	0.6272
A-site[b] total	1.0018	1.0137	1.0027
Fe^{3+}	0.0760	0.0591	0.0782
Al	0.5652	0.5747	0.5572
Cr	1.3551	1.3389	1.3591
Ti	0.0010	0.0010	0.0011
Si	0.0008	0.0126	0.0017
B-site[c] total	1.9982	1.9863	1.9973
End member mol.%			
Chromite ($FeCr_2O_4$)	42.55%	43.70%	42.56%
Magnesiochromite ($MgCr_2O_4$)	24.64%	23.08%	24.85%
Spinel ($MgAl_2O_4$)	10.28%	9.90%	10.19%
Hercynite ($FeAl_2O_4$)	17.75%	18.76%	17.45%
Magnetite ($Fe^{2+}Fe^{3+}{}_2O_4$)	2.39%	1.93%	2.45%
Magnesioferrite ($MgFe_2O_4$)	1.38%	1.02%	1.43%
Others	1.02%	1.61%	1.06%

[a]*Initially, all iron is assumed to be ferrous, and the ferric amount was calculated out based upon assigning four corresponding oxygen atoms pfu.*
[b]*Four-fold coordination positions*
[c]*Six-fold coordination positions*
Detection limits (ppmw): Mg = 0.028, Al = 0.23, Si = 25.6, Ti = 0.13, Cr = 0.13, Mn = 0.048, Fe = 0.93

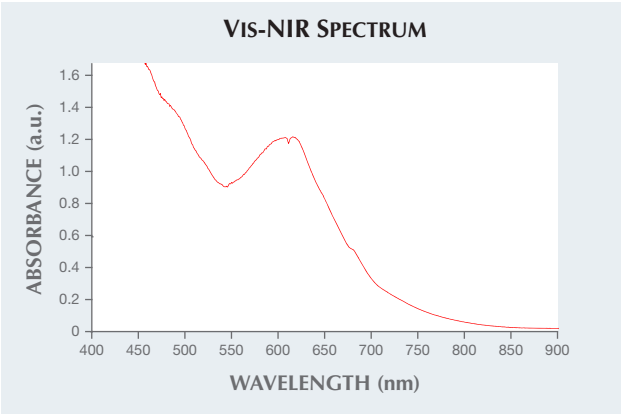

Figure 16. The visible-NIR-range spectrum shows a broad absorption band centered at 610 nm and a smaller band at 680 nm, which may result from minute inclusions of chromium-colored serpentine.

Rare Intense Purplish Pink Montana SAPPHIRE

Recently the Carlsbad laboratory received an intensely saturated purplish pink faceted sapphire for identification and origin report (figure 17). The faceted stone weighed 3.93 ct with measurements of 10.93 × 6.58 × 6.61 mm and had a hexagonal modified mixed-cut style. Standard gemological testing revealed a refractive index of 1.761 to 1.769, and a hydrostatic specific gravity of 3.99, both consistent with corundum. The stone fluoresced medium red to long-wave UV and weak red to short-wave UV.

Figure 17. These Montana sapphires are a 3.93 ct hexagonal modified mixed cut (left, examined for this study) and a 6.39 ct hexagonal rough (right).

Microscopic examination showed angular and oval shaped reflective films, short needles, intact crystals with decrepitation halos and fluid films (figure 18). Also present were dense bands of rutile silk interspersed with finer bands of silk (figure 19). These internal characteristics are typical for sapphires from secondary Montana deposits including Rock Creek, Missouri River, and Dry Cottonwood Creek (E.J. Gübelin and J.I. Koivula, *Photoatlas of Inclusions in Gemstones*, Vol. 3, Opinio Publishers, Basel, Switzerland, 2008, p. 226). The decrepitation halos, the unaltered bands of hexagonal rutile silk, and intact crystals showed no indications of heat treatment. Notably, decrepitation halos are not indicative of heat treatment for sapphires originating from magmatic environments, including Montana sapphires (Winter 2018 Lab Notes, pp. 434–435).

Advanced testing with laser ablation–inductively coupled plasma–mass spectrometry (LA-ICP-MS) was used to obtain the stone's trace element chemistry. The results indicated ranges of Mg (23.8–29.6 ppma), Ti (20.4–22.9 ppma), V (1.75–1.86 ppma), Cr (89.8–108 ppma), Fe (813–864 ppma), and Ga (10.9–11.6 ppma). The LA-ICP-MS trace element chemistry was consistent with Montana sapphires when compared to known sample material from the GIA colored stone reference collection. Chemical profiles for pink and purple sapphires as well as rubies from Montana have been documented (see Winter 2018 Lab Notes, pp. 434–435 and Summer 2019 Gem News International, pp. 286–288).

Figure 18. Reflective decrepitation halos and an unaltered orange crystal. Field of view 1.79 mm.

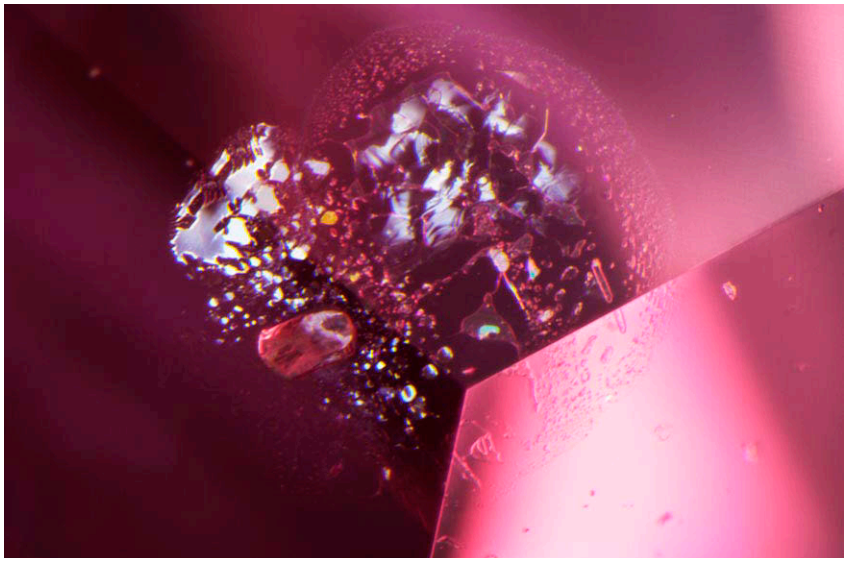

Sapphires from Montana are separated into two groups based on the geology of the deposit. Sapphires from secondary deposits include Rock Creek, Dry Cottonwood Creek, and Missouri River, while the only primary deposit is at Yogo Gulch. The inclusion features in this purplish pink sapphire are consistent with stones from Montana's secondary deposits. This sapphire is reported to be from the Rock Creek deposit. While Rock Creek is historically the most productive deposit in Montana in terms of overall volume of sapphires recovered, stones from this deposit continue to increase in popularity due to their unique colors and excellent clarity (J.C. Zwaan et al., "The origin of Montana's

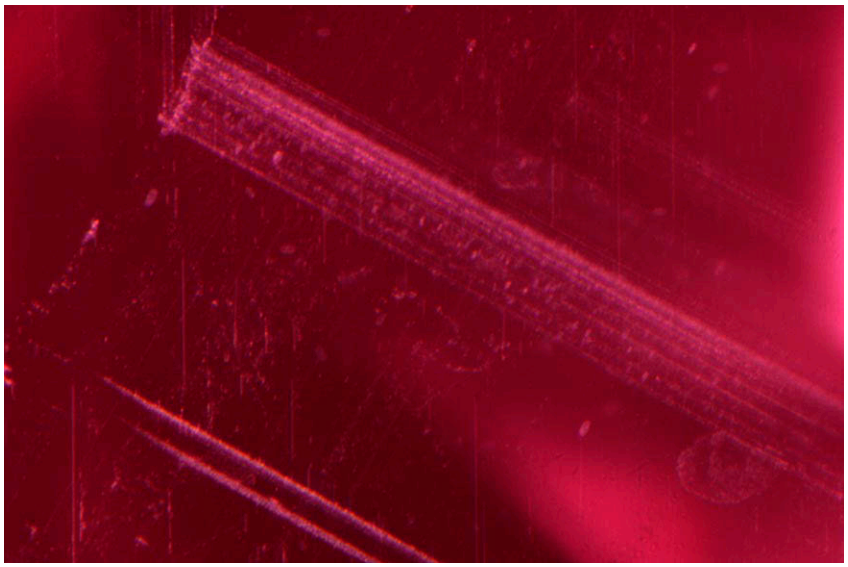

Figure 19. Dense bands of exsolution rutile with finer outer bands frequently seen in secondary Montana sapphires. Field of view 1.79 mm.

Figure 20. This M-color, 7.07 ct round brilliant is the largest CVD-grown diamond seen to date at GIA.

sapphires," Winter 2015 *G&G*, pp. 370–391). Typically, Montana sapphires are less than 2 carats in size. This lends to the rarity and exceptional qualities of this large 3.93 ct intense purplish pink unheated sapphire.

Amy Cooper and Aaron C. Palke

Largest CVD LABORATORY-GROWN DIAMOND Submitted to GIA

Chemical vapor deposition (CVD) diamond growth has greatly improved over the years. More CVD-grown diamonds are seen in the market today, and in recent years, larger CVD-grown diamonds are beginning to emerge. In 2016, the GIA laboratory in Hong Kong examined a 5.19 ct cushion, the largest CVD-grown diamond analyzed at GIA until now (Winter 2016 Lab Notes, pp. 414–416).

A larger CVD-grown diamond was recently submitted to the GIA laboratory in Carlsbad: a round brilliant with VS_2 clarity and M color weighing just over 7 carats (figure 20). This 7.07 ct CVD-grown diamond came to the Carlsbad laboratory undisclosed as CVD, but advanced testing correctly identified this diamond's origin. The largest reported faceted CVD-grown diamond is a 12.75 ct round brilliant ("IGI's Hong Kong lab certifies largest CVD grown diamond," IGI Press Room, November 23, 2020).

Microscopic investigation revealed grade setting graphitic inclusions just below the center of the table. Photoluminescence investigation showed characteristic growth features consistent with a CVD-grown diamond that was subsequently HPHT-treated, generally intended to reduce the brown coloration. With 514 nm excitation at liquid nitrogen temperature (–196°C), nitrogen-vacancy centers at 575 $[NV]^0$ and 637 $[NV]^-$ nm, along with a strong $[SiV]^-$ doublet at 736.6/736.9 nm were revealed (figure 21) determining this diamond as CVD-grown. When viewed through the DiamondView, growth layers were evident (figure 22), and the green fluorescence along with the lack of a 596/597 nm feature in the PL spectrum were indicative of post-

Figure 21. The photoluminescence spectrum collected with a 514 nm laser at liquid nitrogen temperature reveals the NV centers and silicon-vacancy center that are typically observed in CVD-grown diamonds.

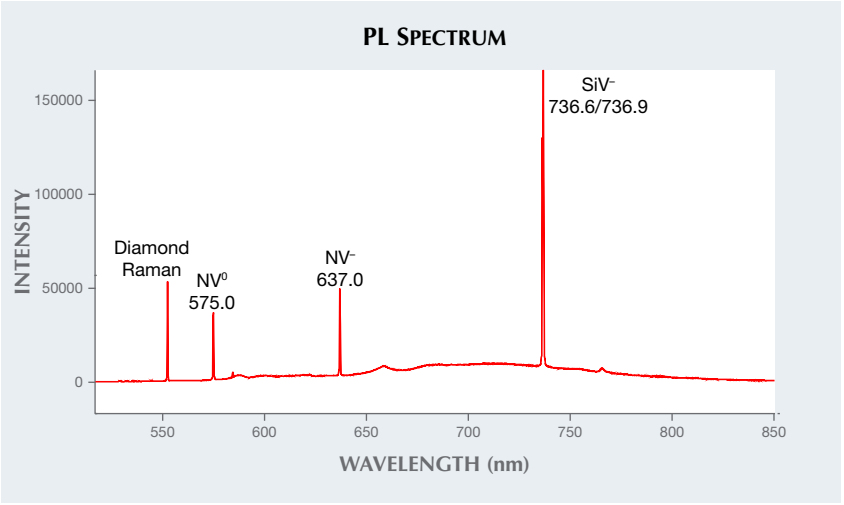

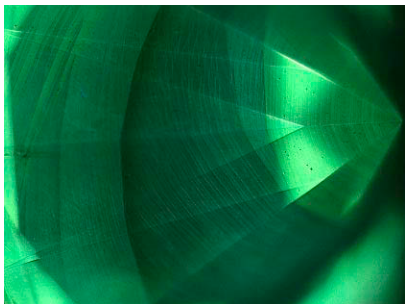

Figure 22. DiamondView fluorescence imaging shows the striations that are diagnostic of its CVD origin, and its coloring is consistent with post-growth HPHT treatment.

growth HPHT treatment (figure 22; Wang et al., "CVD synthetic diamonds from Gemesis Corp.," Summer 2012 *G&G*, pp. 80–97).

CVD-grown diamonds of these sizes are still a rarity, but with new technologies and advancements it is evident that larger laboratory-grown diamonds are becoming more prevalent.

Garrett McElhenny and Sally Eaton-Magaña

Unusual Absorption in a Blue Flux-Grown SYNTHETIC SAPPHIRE

The GIA laboratory in Bangkok analyzed a 0.52 ct blue flux-grown synthetic sapphire (figure 23). Standard gemological properties were typical for corundum. Observation in the microscope revealed various forms of flux or wispy fingerprints and platinum inclusions in a variety of shapes (figure 24). All of these inclusions are typical for Chatham synthetic sapphire (R. Kane, "The gemological properties of Chatham flux-grown synthetic orange sapphire and synthetic blue sapphire," Fall 1982 *G&G*, pp. 140–153).

Figure 23. A 0.52 ct blue flux-grown synthetic sapphire.

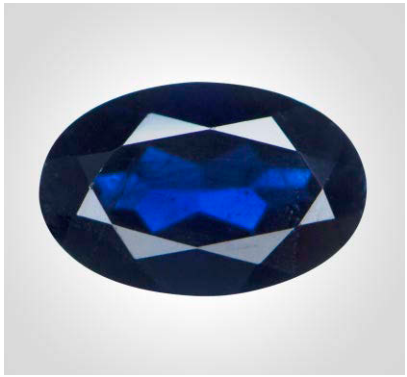

Figure 24. Platinum inclusions in a variety of shapes.

However, the most interesting feature of this stone was its UV-Vis-NIR spectrum (figure 25). The spectrum had the usual 377, 388, and 450 nm peaks related to Fe^{3+}, as well as the Fe^{2+}-Ti^{4+} broad band around 560 nm that is responsible for the blue color, but additionally featured an unexpected broad band around 800 nm. The broad band at 800 nm is typ-

Figure 25. UV-Vis-NIR spectra of faceted blue flux-grown synthetic sapphire. Estimated path length 2.51 mm.

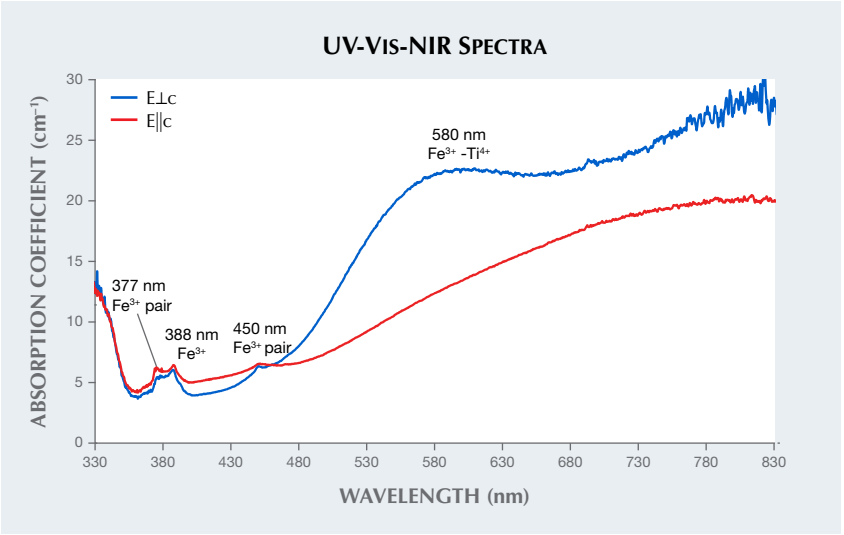

TABLE 2. LA-ICP-MS results in parts per million atomic (ppma) for the blue flux-grown synthetic sapphire.

	Be	Mg	Ti	V	Cr	Fe	Ga	Rh	Pt
Average	12.2	0.083	95	0.025	0.99	1299	0.51	1.3	1.08
SD (n = 3)	0.8	0.001	8	0.002	0.02	37	0.03	0.1	0.05
Detection limit	0.07	0.025	0.07	0.007	0.08	1	0.004	0.0004	0.001

ical for basalt-related, natural blue sapphire and can also be found in some heated metamorphic blue sapphire (Summer 2019 *G&G* Micro-World, pp. 264–265). However, it has never been reported in blue lab-grown sapphire, either flame-fusion or flux-grown.

We analyzed the trace element composition on the blue flux-grown synthetic sapphire using LA-ICP-MS. The results showed very low amounts of vanadium (V) and gallium (Ga), a combination that is a classic indicator of lab-grown corundum. Other trace elements such as titanium and iron were found at levels on average of about 95 ppma and 1299 ppma. Beryllium was also detected at 12 ppma (table 2), a trace element whose presence is unpredictable in laboratory-grown sapphire. The presence of rhodium (Rh) and platinum (Pt) is an indicator of flux-grown corundum, representing traces of the crucible in which the sapphire was grown.

Sudarat Saeseaw

PHOTO CREDITS
Diego Sanchez—1, 8, 9, 12, 20; Britni LeCroy—2; Virginia Schwartz—3; Jian Xin (Jae) Liao—4; Nathan Renfro—10, 13, 15, 18, 19; Angelica Sanchez—14, 17; Adam Steenbock—22; Nuttapol Kitdee—23; Charuwan Khowpong—24